Effects of leaching and chloride migration on the microstructure and pore solution of blended cement pastes during a migration test

Rachid Cherif, Ameur El Amine Hamami, Abdelkarim Aît-Mokhtar

Effects of leaching and chloride migration on the microstructure and pore solution of blended cement pastes during a migration test

Rachid Cherif*, Ameur El Amine Hamami, Abdelkarim Aït-Mokhtar

LaSIE UMR CNRS 7356, University of La Rochelle, Avenue Michel Crépeau, 17042 La Rochelle Cedex 1, France

Abstract

This paper investigates the influence of the multispecies diffusion and leaching phenomena on the thermodynamic equilibrium and microstructure of cementitious materials containing mineral additions during a chloride migration test. Because of a lack of data on these effects, the aim of this study was to quantify changes in the material's microstructure during an experimental program based on mercury intrusion porosimetry before and after chloride exposure, scanning electron microscopy and chemical analyses of the materials. The experimental results highlight a modification of pore size distribution and a reduction of up to 60% in total porosity after chloride transfer. This was due to chloride interactions which led to the formation of new compounds in the porosity range of 7 to 70 nm. These compounds were investigated by elemental analyses and quantified.

Moreover, a chloride migration test was performed in order to investigate the leaching of pore solution ions in the two compartments of the migration cell. The results enabled us to: (i) quantify the concentration of ions that diffused into/from the material, and (ii) estimate the kinetics of calcium release and the quantity of portlandite dissolved in the material. The chloride diffusion coefficient of the materials ranged between 2.38×10^{-12} and 5.96×10^{-12} m²/s, the kinetics of calcium, expressed as a flux, were between 1.8×10^{-2} and 1.2×10^{-1} mmol.m^{-2}.s^{-1}.

Keywords: cement pastes, pore size distribution, chlorides, multispecies transfer, thermodynamic equilibrium, leaching.

*** Corresponding author:**
e-mail address: rachid.cherif@univ-lr.fr
Tel: +33 5.46.45.72.30.

HIGHLIGHTS

- Chloride migration induced porosity changes in cement pastes with different pozzolanic materials and limestone that could reach 60%.
- During chloride migration, new salts occupy the porosity of cement pastes used in the range 7– 70 nm.
- The kinetics of calcium release, expressed as a flux, ranged from $1.8x10^{-2}$ to $1.2x10^{-1}$ $mmol.m^{-2}.s^{-1}$.

1. Introduction

The durability of reinforced concrete structures is governed by the mechanical behavior of the materials used and vice-versa. Durability is also affected by environmental attacks, in particular by aggressive species present in the environment of the structures [1–6]. This phenomenon leads to the corrosion of rebar steel and damage to concrete [7,8]. The aggressive species studied in the literature are mainly carbon dioxide, marine or de-icing salts and sulfates. The present work focused on chloride ion transport through cementitious materials.

During ionic transport, chlorides interact chemically with anhydrous compounds in cement (chemical interactions) [9,10]. Chlorides can also be adsorbed by the C- S- H layers (electrochemical interactions and electrical double layer) [11,12]. Indeed, the chemical interactions produce compounds that precipitate in the pore solution and modify the porosity and pore size distribution of the material, as has been demonstrated in the carbonation of cementitious materials [13,14], and this can even induce cracking [15]. In terms of the chemical composition of the pore solution, external ions such as chlorides generate a thermodynamic imbalance in the hydrates/pore solution system, promote the dissolution of portlandite [16], [17] and the precipitation of compounds such as Friedel's and Kuzel's salts [6,18,19].

Qiao *et al*. [6] quantified the Friedel's salt formed in the porosity of cement-based materials during chloride transfer and its influence on the mechanical properties (flexural strength) due to crystallization pressure. Furthermore, Midgley and Illston [20] and Kayyali [21] monitored the porosity of Portland cement pastes after 28 and 90 days of immersion in sodium chloride solutions (30 and 39 g/l respectively). They showed that chlorides reduced and refined the porosity due to the formation of calcium chloride on the surface of C-S-H. Regourd *et al.* [22] reported that chlorides changed the initially fibrous C-S-H to a reticulated morphology. In addition, Koleva *et al*. [23] measured the pore size distribution of mortars partially immersed in a 7% NaCl solution. The results showed that chloride diffusion into the fully immersed part of the material decreased its total porosity and refined the pore network. Sutter *et al*. [10] reported a formation of calcium oxychloride in the porosity of mortar specimens immersed in a 15% $MgCl_2$ solution. This modification of the microstructure influences the intrinsic permeability [23] of the material and its chloride diffusion coefficient. Finally, Hu *et al*. [24] immersed samples of cement in a NaCl solution (0.1 to 1.0 mol/l). Their investigations showed that the chloride concentration index and Zeta potential decrease with the concentration of the soaking solution.

More recently, Electrochemical Impedance Spectroscopy (EIS) has been used as a powerful technique to study the microstructure and mechanical properties of cementitious materials [25–27]. This technique can be used to correlate the dielectric response and the characteristics of the material. Sanchez *et al.*[27] used EIS to monitor the microstructural changes of concrete in real time during a chloride migration test from the beginning (non-steady state) until the steady state was reached. The authors noted that the dielectric response of concrete was strongly modified during the chloride migration test and that these modifications were due to microstructural changes in the concrete. Indeed, during the first stages of chloride migration, resistance decreased to a minimum value (180 Ω) when the material was completely saturated

with chlorides. In addition, the capacity values remained low and constant during the first 100 - 200 hours. No modification in the microstructure was observed, only the pore solution changed. After an average of 200 hours, an increase in resistance and capacity was recorded. This was explained by a reduction in total porosity and an increase in tortuosity due to the formation of new compounds in the porosity. Subsequently, these dielectric parameters became constant at the steady state.

In reality, chlorides penetrate into concrete by natural diffusion under total immersion in water or by diffusion and convection for partial immersion, e.g. in the tidal phenomenon. Diffusion is a very slow phenomenon for investigations in the laboratory compared to accelerated chloride migration. Several researchers [28–30] have discussed the difference between chloride diffusion (what is really happening) and accelerated diffusion (i.e. migration) due to the presence of a counter electrical field. In this sense, several theoretical relationships between chloride diffusion and migration coefficients have been proposed [28,31]. In general, accelerated diffusion does not exist, but remains a simple and rapid way to estimate the chloride diffusion coefficient as well as the influence of chloride on microstructure in the lab [27,32].

These studies only focused on the causes of microstructure changes during chloride transfer due to the precipitation of new compounds. The latter were not quantified. The physico-chemical process of the dissolution/precipitation phenomena was not investigated to explain these microstructural changes. To our knowledge, there are few studies on the change in thermodynamic equilibrium induced by chloride diffusion, or the quantification of new species derived from the dissolution or precipitation of compounds to reach a new equilibrium in the thermodynamic system.

Moreover, numerical models for simulating chloride transfer have been developed from Fick's law [33,34] and, more recently, from the Nernst-Planck equation [35–38]. Often, these models

do not take into account the porosity or pore size distribution induced by chloride transfer because of a lack of data and the complexity in modeling this phenomenon.

Therefore, the aim of this study was to investigate the changes in both microstructure and pore solution of cement paste samples exposed to a NaCl solution. These changes are investigated MIP before and after migration tests, along with image processing from scanning electron microscopy (SEM). The objective was to characterize pore size modification and then to identify and quantify the compounds responsible for the change in porosity, apart from known salts like Friedel's.

In addition, chemical analyses of the pore solution and upstream and downstream analyses of the migration cell were performed to identify the species diffusing into/out of the material during a migration test. Thus, we could quantify the species that leached from the sample, and monitor the kinetics and degree of portlandite dissolution, which is responsible for the stabilization of the thermodynamic equilibrium. These phenomena modify the pore solution and microstructure and affect chloride transport conditions.

2. Experimental approach

2.1. Materials

An ordinary European Standard (NF EN 197- 1) Portland cement "CEMI 52.5 N" was used [39]. The mass fractions of the principal clinker phases provided by the manufacturer (Calcia, Bussac-France) and based on the Bogue calculation method are 65% C_3S, 13% C_2S, 7% C_3A, 13% C_4AF and 4.9% gypsum. Furthermore, pozzolanic materials and limestone (limestone filler "LF", fly ash "FA", blast furnace slag "S" and silica fume "SF") were used as a mass substituent of the cement. The chemical composition, density and Blaine specific surface area (BSSA) of the cement and the different additions used are given in Table 1.

Table 1. Chemical composition and physical properties of materials used

Composition	CaO	SiO_2	Al_2O_3	Fe_2O_3	SO_3	K_2O	Na_2O	Chlorides	Density	BSSA(m^2/kg)
CEM I (wt.%)	64.20	20.50	5.00	3.90	2.50	0.29	0.05	1.40	3.18	405
LF (wt.%)	98.80	0.30	0	0	0.01	0.01		0.001	2.70	498
FA (wt.%)	5.10		85.53		0.59	2.00	1.95	0.013	2.21	405
Slag (wt.%)	41.50	33.30	12.50	0.40	0.50	0	0	0	2.89	450
SF (wt.%)	1.00	89.00	0	0	2.00	0	1.00	0.10	2.24	-

Firstly, a reference concrete based on CEM I 52.5 N was formulated following the Dreux-Gorisse method, with an average compressive strength f_{cm} of 38 MPa. A fixed amount of cement of 300 kg/m^3 was used. Then, we formulated other concretes containing pozzolanic materials and limestone using an approach similar to that used by Khokhar *et al.* [40] and Younsi *et al.* [41], keeping the paste volume (V_p) constant and equal to that of the reference concrete (V_P = 24.5% of the total volume). This approach is based on solving a system of equations for 5 unknowns: V_G, V_S, V_C, V_A and V_w that are volumes of gravel, sand, cement, additions and water, respectively. The total volume of concrete was 0.975 m^3 (considering a volume of air of 0.025 m^3). The system of equations is as follows:

$$\begin{cases} V_G + V_S + V_C + V_A + V_W = 0.975\ m^3 \\ \dfrac{V_G}{V_S} = x \\ \dfrac{A}{C+A} = y \\ V_C + V_A + V_W = V_p \\ f_{cm} = 0.5\sigma\left(\dfrac{C+kA}{W} - 0.5\right) \end{cases} \quad (1)$$

where (σ=52.5MPa) is the cement resistance, C, A and W are the masses in (kg) of cement, additions and water, respectively. The last equation (Bolomey relation) links f_{cm} and the W/B (Water/Binder) ratios by taking into account the coefficient of chemical activity "k" of each addition ($B = C + kA$). This causes a difference between the W/B of the formulated materials. The properties of the formulated concrete pastes were used to manufacture the cement pastes

studied in this work. Investigations on cement pastes are easier than on concretes, mainly for pore solution extraction, thanks to the higher porosity of the cement paste.

Five cement pastes were used: the reference cement paste without additions is called PCI, while those containing different pozzolanic materials and limestone are called LF25 (25% of Limestone Filler), FA30 (30% of fly ash), S75 (75% of blast furnace slag) and SF10 (10% of silica fume) respectively. Table 2 gives the W/B ratios of the cement pastes tested.

Table 2. W/B ratio of cement pastes used.

Material	PCI	LF25	FA30	S75	SF10
W/B	0.50	0.38	0.40	0.44	0.47

The choice of these additions and their ratios of cement replacement are justified as follows: 75% of blast furnace slag brings major modifications to the microstructure of cementitious materials and chloride diffusivity, particularly the chemical and electrochemical fixation of chlorides on the C-S-H layers [42]. Fraay *et al*. [43] demonstrated that for the mass replacement of cement by more than 30% of fly ash, only 50% of the latter reacts at the end of the first year. According to Perraton *et al*. [44], it is preferable to substitute between 5 and 10% of the mass of cement with silica fume; above 10%, the replacement is useless and the performance of the material decreases.

Cylindrical specimens (11cm diameter and 22cm height) were cast and demoulded 24 hours after manufacturing and cured for 365 days in an alkaline solution composed of 25 mmol/l NaOH and 83 mmol/l KOH to reduce leaching [26,45]. Afterward, the samples used in the migration test were obtained from these specimens by coring samples from the heart and saw cutting to obtain discs 6.3 cm in diameter and 2.8 cm thick.

2.2. Tests and procedures

Cement paste samples, aged 1 year, were subjected to migration tests for 12 - 14 days. This period corresponds to the time required to achieve a steady state of chloride migration. Pore size distribution was determined before and after each migration test. For a better representativeness, samples used for pore size distribution before chloride migration were taken in the neighborhood of the sample used for the migration test. At the end of the migration test, samples were cut off manually from the disc for an MIP test (mercury porosity, pore size distribution and critical pore diameter) and SEM analyses (see details of the performed tests in Fig. 1). A steady-state chloride migration test was used in order to quantify more precisely the complete change induced by the test. While in a non-steady state, modifications always take place while measurements are being made to calculate the apparent diffusion coefficient. Quantifying these modifications is then difficult to achieve.

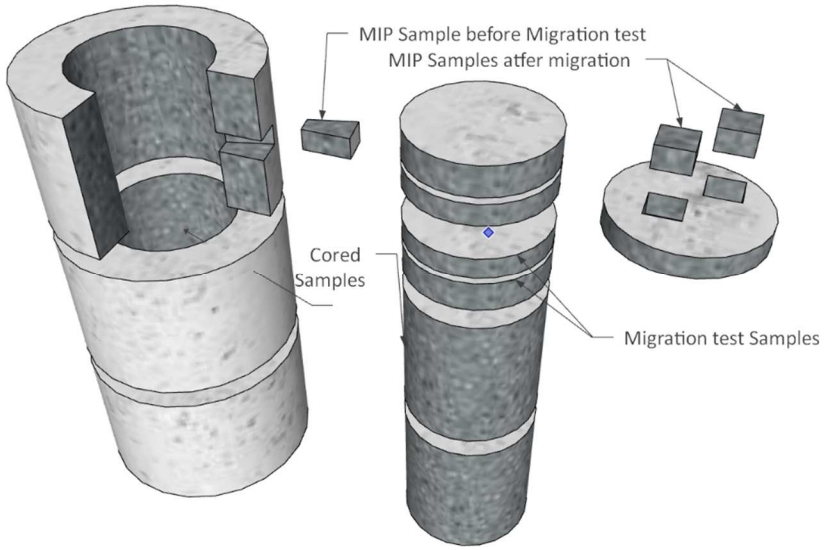

Fig. 1. Schematic representation of specimens sampled for studying the influence of chloride migration on the microstructure of cement pastes.

2.2.1. Water and mercury porosimetry

The water porosity of the cement pastes was measured by hydrostatic weighing according to the French NFP 18-459 standard [46]. The weighing scale used was accurate down to 1 mg. The water porosity was calculated using eq. (2).

$$\varepsilon = \frac{M_{sat} - M_{dry}}{M_{sat} - M_{water}} \times 100 \quad (2)$$

where, M_{sat} is the mass of the saturated sample, M_{dry} is the mass of the dried sample and M_{water} is the mass of the saturated specimen immersed in water (obtained by hydrostatic weighing).

MIP measurements were performed with an Autopore III 9420 from Micrometrics® whose pressure limit is more than 400 MPa; it covers pore diameters from 3 nm to 360 µm. Some authors [47,48] have suggested that this technique is not optimal for measuring pore size distribution. Nevertheless, it remains widely used [27,49]. Prior to the test, the samples were first dried at 45°C under a vacuum until mass stabilization. The main advantage of using this temperature is that it avoids cracking and delays ettringites formation [50]. The samples were cut off manually, avoiding the use of a saw, which can modify the sample's microstructure.

2.2.2. Migration test

The method developed by Aït-Mokhtar *et al.*[51] was used. The objective was to determine the effective chloride diffusion coefficient in the steady state. An electrical field of 300 V/m was applied between the two sides of the saturated sample. This value was chosen to avoid the Joule effect, temperature increase and sample degradation [9,27,30,52]. A support solution based on 25 mmol/l of NaOH and 83 mmol/l of KOH was used in the upstream and downstream compartments of the migration cell to simulate the pore solution of cementitious materials [26,45]. NaCl was added to the upstream solution at a concentration of 500 mmol/l. The compartment solutions were renewed every 24 hours, without taking into account changes in their concentration, in order to keep the same boundary conditions on both sides of the specimens during the migration test. The solutions in the compartments were analyzed before each renewal in order to monitor diffusion/leaching kinetics. The effective chloride diffusion coefficient D_{eff} (m/s²) was calculated using eq.(2) [53].

$$D_{eff} = \frac{RTL}{z_{Cl^-}FU}\frac{J}{C_{up}}\left(1 - e^{\frac{z_{Cl^-}}{RT}FU}\right) \quad (2)$$

where L (m) is the thickness of the sample; C_{up} (mol/m^3) the concentration of chloride ions in the upstream solution; U (V) the potential difference at the sample terminals; F, z_{Cl^-}, R and T represent the Faraday constant, the valence of the chloride ion, the ideal gas constant and the absolute temperature (K); J is the chloride flux.

2.2.3. Analyzes of solutions with ionic chromatography (IC)

The upstream and downstream solutions of the migration cell were regularly analyzed. In addition, the initial concentration of calcium and sulfates in the pore solution of the material (before the migration test) were dosed and compared to those that leached into the two compartments during the migration test. Chemical analyses were performed using a "883Basic Ion Chromatograph Plus" from Metrohm®. Note that for the upstream solution, dilutions of 1:1800, 1:150, 1:40 and 1:1 were necessary to dose sodium, potassium, calcium and sulfates, respectively. The downstream solution required a 1:150 dilution to dose sodium and potassium and 1:1 for calcium and sulfates.

2.2.4. Extraction of the pore solution samples

The pore solution of the cement pastes was extracted using an OpiCAD® device according to a procedure previously described [54,55]. The cement paste sample, with a volume of 137 cm^3, was placed in a cylindrical chamber underneath a piston. The piston was loaded using a standard compression test machine. In order to obtain an optimal performance and take into account the creep effects, two steps were conducted. First, the samples were loaded at a constant loading velocity of about 0.02 MPa/s for 15 minutes. This first step was followed by a 5 minutes idle phase. Finally, the solution was collected from the bottom of the cylindrical chamber and analyzed by ionic chromatography.

2.2.5. Scanning Electron Microscopy (SEM)

The microstructure of the tested samples was analyzed by scanning electron microscopy (SEM) in environmental mode before and after chloride migration. The advantage of this mode is that no preparation is required and no coverage is deposited on the surface of the specimens, which avoids disturbing the morphology and the microstructure of the sample. Also, the MEB test was performed on manually fractured samples immediately at the end of the migration test. This avoids using a concrete saw and preserves the microstructure and chemical composition of the surface of the specimens. Furthermore, to measure the elemental distribution of precipitated compounds at the microscopic level, energy dispersive X-ray micro-analysis (EDX) was coupled to the SEM analyses.

3. Results and Discussion

3.1. Diffusion coefficient and water porosity

Fig. 2 shows the water porosity and its standard deviation from three measurements of the cement pastes. PCI had the highest porosity compared to the other pastes. This is mainly due to the higher W/B ratio of PCI compared to LF25, FA30, S75 and SF10 (see Table 2). Furthermore, the use of 10% silica fume should decrease the porosity as long as it is compared to pastes with the same W/B ratios [56]. However, the W/B ratio of SF10 is higher than the other cement pastes with pozzolanic additions and a filler, which is why the total porosity of the cement pastes used was relatively similar. LF25 has a low W/B ratio and thus a relatively low porosity.

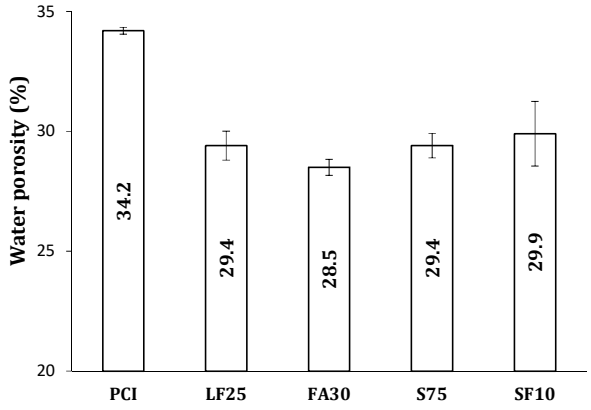

Fig. 2. Porosity of cement pastes.

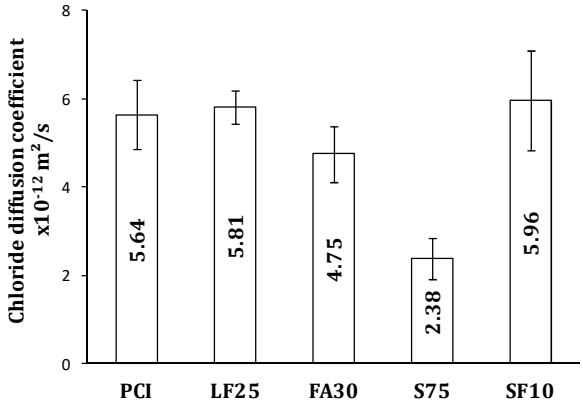

Fig. 3. Chloride diffusion coefficient of cement pastes.

Fig. 3 gives the chloride diffusion coefficient and its standard deviation from three measurements of the cement pastes. The results show that S75 had the lowest chloride diffusion coefficient compared to the other cement pastes. This is due to the replacement of Portland cement by 75% of blast furnace slag, which refines the microstructure. Indeed, a finer microstructure increases the electrochemical fixation of chlorides at the pore-solution interface of the material, which slows down diffusivity [42]. Despite the use of pozzolanic materials such as silica fume (SF), which are finer than cement and are supposed to reduce the diffusion coefficient [57], the results show that the chloride diffusion coefficients of PCI, LF25, FA30 and SF10 were of the same order of magnitude. The difference observed can be attributed to the mixing of the cement pastes without vibration and without a superplasticizer, which generates a non-optimized microstructure. The low W/B ratio of SF10 is a disadvantage for the non-optimization of the microstructure, taking into account the high-water demand for silica fumes.

3.2. Influence of chlorides on the microstructure of the cement pastes

Fig. 4 illustrates the mercury porosity values before and after the chloride migration tests. After migration, a reduction in porosity was noticed for all the materials, with ratios of 2.5, 2.1, 2.2, 1.6 and 1.4 for PCI, LF25, FA30, S75 and SF10, respectively. This reduction is due to the

formation of new chloride-based compounds in the porosity such as Friedel's and Kuzel's salt [6,19], and calcium oxychloride [10].

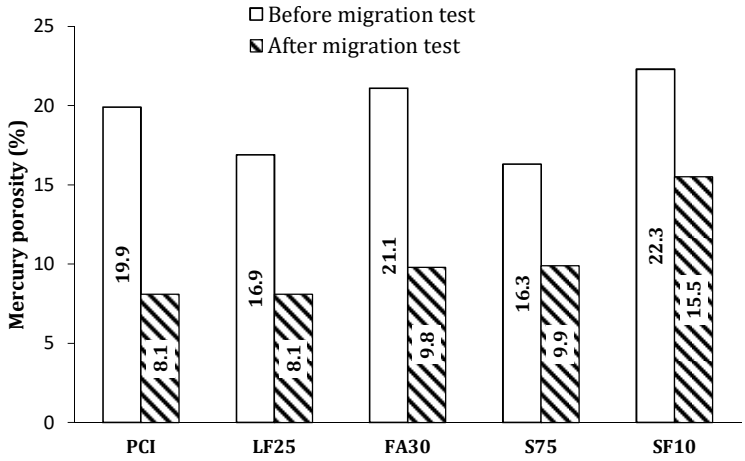

Fig. 4. Mercury porosity of cement pastes before and after the migration test.

In addition, Fig. 5 illustrates the pore size distribution obtained by MIP before and after the migration tests. Before the migration tests, the pore size distribution of the cement pastes was generally monomodal. The critical pore diameters were located around 69 nm for PCI, 50 nm for LF25, 45 nm for FA30 and 69 nm for SF10. However, with about 8 nm, the S75 critical pore diameter was the smallest. This is in agreement with previously published results [42]. After chloride migration, there were changes in pore size distribution and a shift in critical diameter peaks.

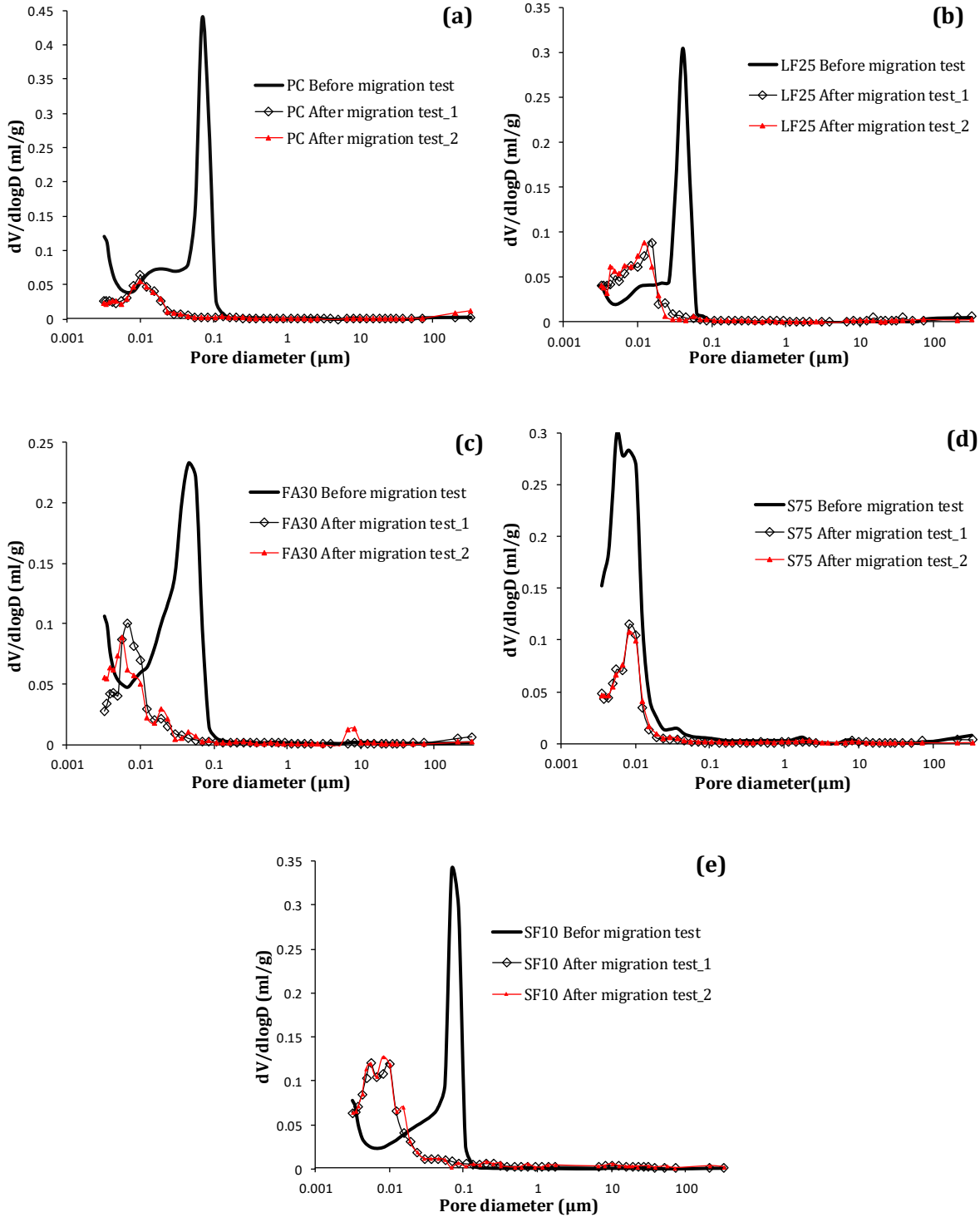

Fig. 5. Pore size distribution before and after the chloride migration test.
(a) PCI; (b) LF25; (c) FA 30; (d) S75 and (e) SF10.

Fig. 6 illustrates the reduction rate of the critical pore diameter. After the migration test, there was a decrease in the critical pore diameter for PCI, LF25, FA30 and SF10 ranging between 70% - 88%, showing a refinement of porosity. This reduction is reflected by the decrease in the

number of large pores and the increase in the number of fine pores [32,58]. However, S75 highlighted the changes in pore size distribution and porosity, but its critical diameter remained constant. The latter was too small to contain new compounds, which require more space [59]. These microstructure changes affect transport properties such as air or water permeability.

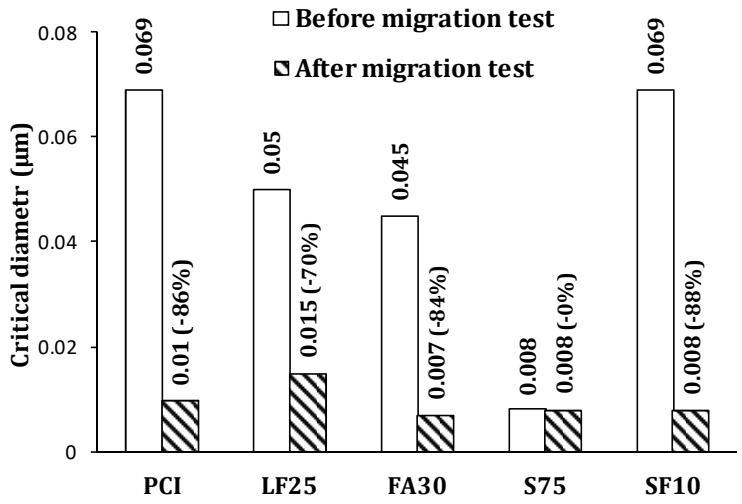

Fig. 6. Critical pore diameter of cement pastes before and after the migration test.

In general, cement hydrates form a basic pore solution composed mainly of sodium, potassium and hydroxyl [60]. The exposure of cementitious materials to saline environments generates an imbalance in the hydrates/pore solution thermodynamic system due to chloride diffusion and leaching of the pore solution ions. This imbalance induces some hydrate dissolution to stabilize the system [61]. For instance, Chatterji [16] showed that chloride transfer is accompanied by the formation of salts, providing compounds in the form of (C_3A $CaCl_2$ x H_2O). Furthermore, Monosi and Collepardi [62] and Sutter *et al.* [10] showed that chlorides induce the precipitation of hydrated calcium oxychloride ($3CaO$ $CaCl_2$ $15H_2O$) in the porosity and a consumption of portlandite according to reaction (1). They noted the precipitation of Friedel's salt ($3CaO{\cdot}Al_2O_3{\cdot}CaCl_2{\cdot}10H_2O$) in the porosity of the same specimens and showed that calcium oxychloride and Friedel's salt can occur together.

$$3Ca(OH)_2 + CaCl_2 + 12H_2O \rightarrow 3CaO \cdot CaCl_2 \cdot 15H_2O \quad (1)$$

In general, the refinement in porosity due to the precipitation of new salts during chloride transfer can influence the measurement of the diffusion coefficient, mainly for a migration test in a non-steady state, where the chemical interactions and the precipitation phenomena are not completed. The crystallization of these salts can generate cracks, principally in materials with low porosities [59]. Therefore, this influences the estimation of the diffusion coefficient. If the steady state test is used, the microstructure modification will have already taken place. There is a constant flow of chlorides downstream and the calculated diffusion coefficient is that of the modified material.

In order to quantify the chemical composition of these newly formed salts, apart from known ones such as Friedel's salt, we used SEM analyses to investigate the surface characteristics and microstructure of the hardened cement pastes, before and after the migration tests. A comparison between the SEM Images of healthy materials and those exposed to chloride migration is shown in Fig. 7 to Fig. 9 (For PCI, FA30 and S75, respectively). Figs 7a, 8a and 9a show the healthy materials, and Figs 7b, 8b and 9b show the materials exposed to chlorides. The corresponding EDX spectra, with a precision of 10^{-2}, are also given. Note that the location of these investigated areas was chosen in wall pores where new chloride-based compounds are formed. This allowed us to quantify the species that make up these salts.

For PCI, X-ray analyses showed new chloride-based precipitates in the porosity after the migration tests. We also observed sulfides, which could confirm the possible formation of monosulfoaluminates (AFm) and trisulfoaluminates (AFt) in the porosity. Indeed, Famy *et al.* [63] showed that sulfates are physically adsorbed by the C-S-H layers. The presence of calcium and alkalis in the pore solution increases the quantity of sulfates adsorbed [50]. That is why leaching alkalis and calcium affect the release of sulfates and then the precipitation/dissolution

of AFm and AFt [61,64]. Moreover, Marcotte *et al.* [58] showed that ionic migration through concrete leads to the partial decomposition of some hydrates such as C-S-H and AFm. Therefore, different ions such as Ca^{2+}, OH^- and SO_4^{2-} can be released in the pore solution. These species may participate in the precipitation of salts in larger pores. This phenomenon could be projected to the transfer of chlorides in general. Furthermore, potassium in a solid form was observed in materials after the migration tests (Table 3). Unfortunately, we did not follow this reaction. This was probably due to a precipitation of KCl. However, at this stage, we have no justification for this phenomenon. More chemical investigations will be necessary to elucidate the reaction responsible for the potassium precipitation.

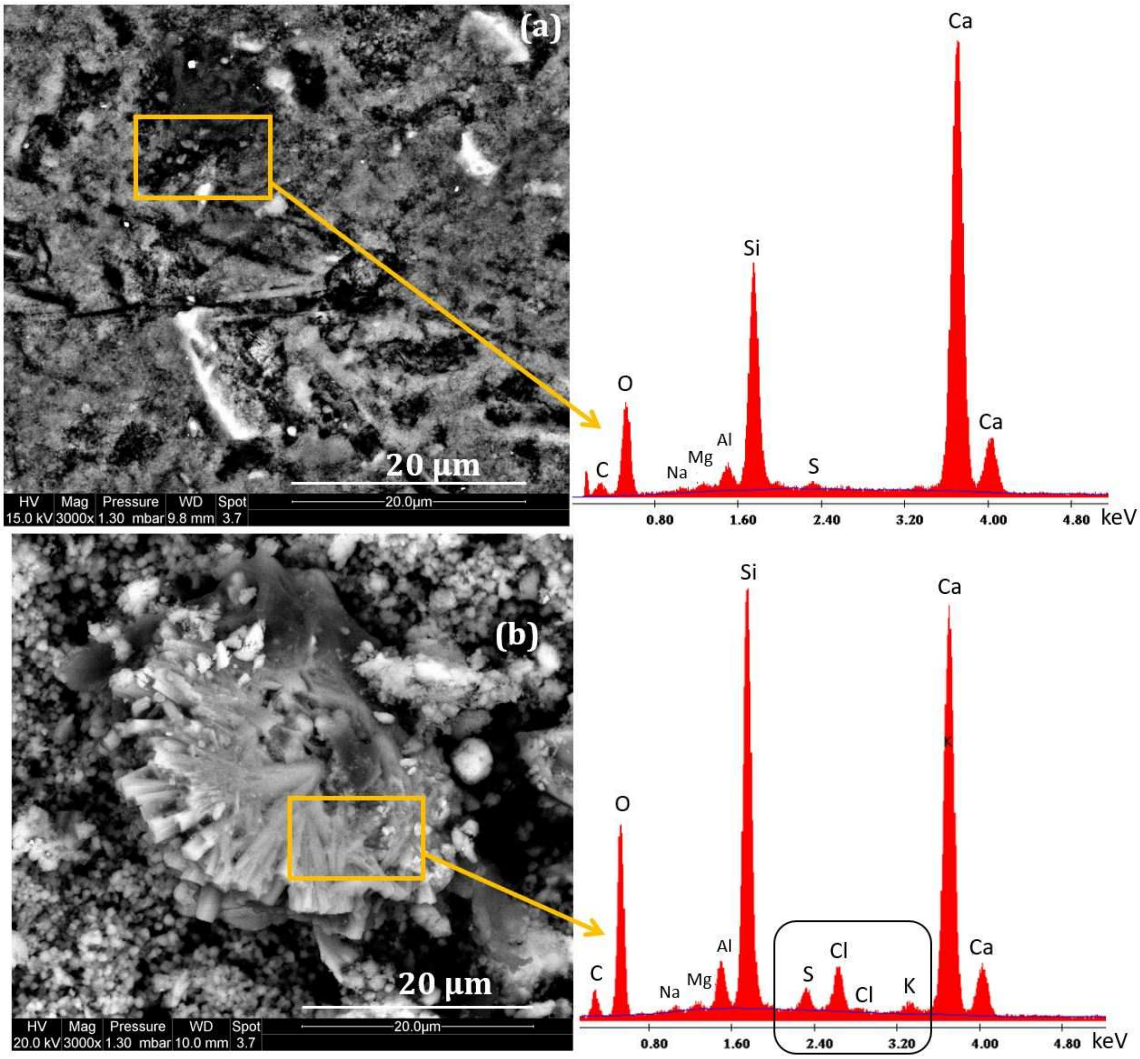

Fig. 7. SEM images and EDX spectra of PCI: (a) before and (b) after the migration test.

Table 3 shows the mass fraction of elements corresponding to the spectra. It represents a comparison between the weights of the chemical elements in the solid part analyzed before and after the migration of chlorides. This gives information on the elemental distribution of the new compounds formed.

Table 3. Chemical species detected in the vicinity of pores of PCI (% in weight)

Element	C	O	Na	Mg	Al	Si	S	Ca	Cl	K
Before migration test	7.17	33.88	0.78	0.84	1.72	13.43	0.50	40.14	0	0
After migration test	9.33	38.40	0.42	0.43	2.13	16.98	1.08	26.88	2.41	0.70

Fig. 8 highlights chlorides (1.71%), sulfide (0.63%), sodium (1.03%) and potassium (1.61%) in solid form in the porosity of FA30 subjected to migration tests; these species were not present in solid form before the tests. The quantity of these species is given in Table 4.

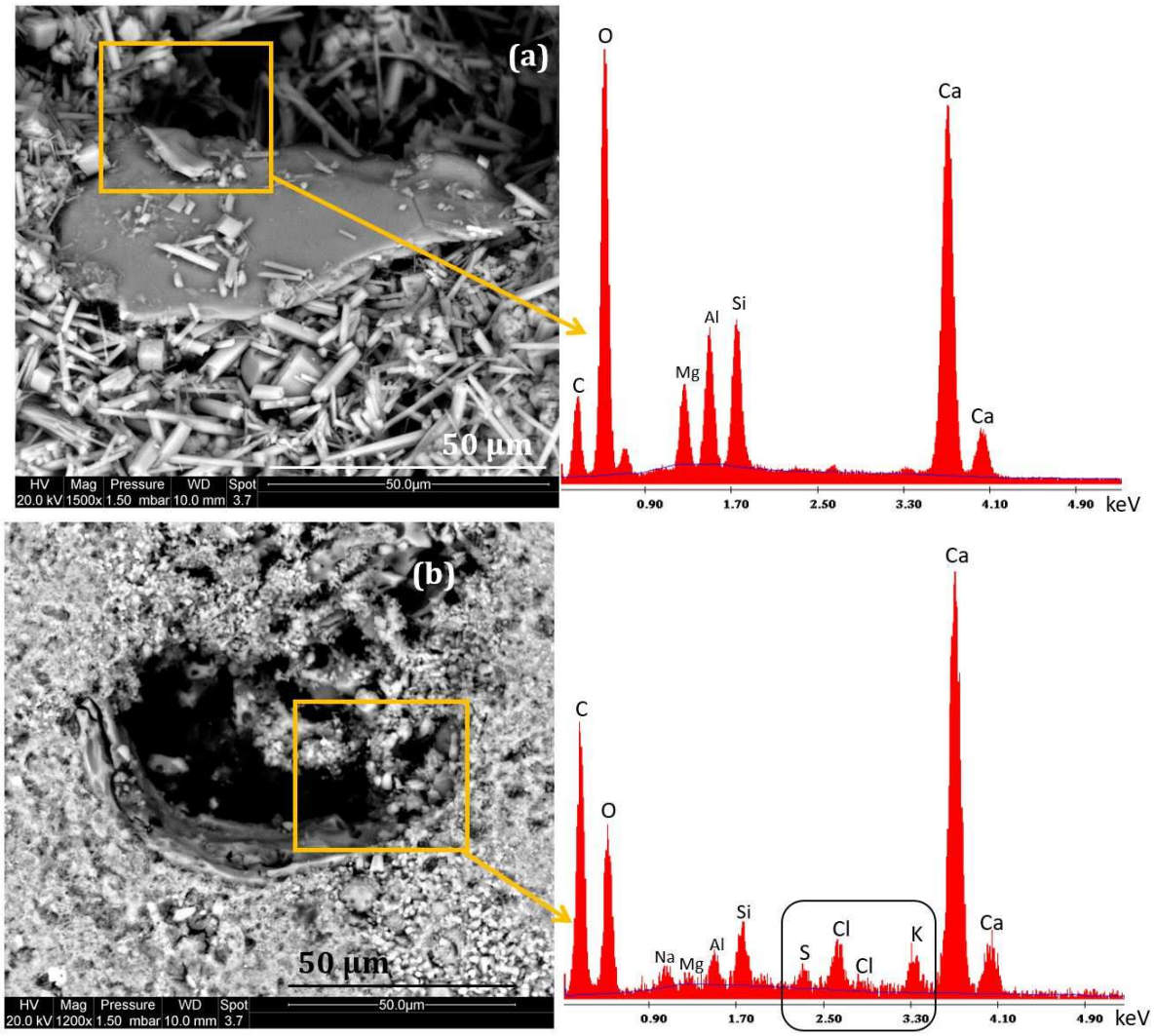

Fig. 8.SEM images and EDX spectra of FA30: (a) before and (b) after the migration test.

Table 4. Chemical species detected in the vicinity of FA30 pores (% in weight)

Element	C	O	Na	Mg	Al	Si	S	Ca	Cl	K
Before migration test	17.89	45.60	0	3.18	4.47	4.66	0	16.35	0	0
After migration test	44.60	27.45	1.03	0.32	1.05	1.75	0.63	19.21	1.71	1.61

The spectra in Fig. 9 give the chemical composition of the investigation area of S75 before and after the migration tests. After the tests, the spectrum of S75, whose microstructure has fine pores, highlights the low chloride content: 0.68% in weight for S75 (Table 5) compared to 2.41% and 1.71% for PCI and FA30, respectively. This result confirms that new chloride based compounds precipitate more easily in large pores [59]. The chemical composition of S75 presented in Table 5 is in agreement with that of PCI and FA30. Finally, the amount of carbon

noted for the three measurements is certainly due to the preparation and handling of the sample before MEB analyses (see section 2.2.5). There is no risk of carbonation in the MEB chamber with the environmental mode since the vacuum pump does not contain oil.

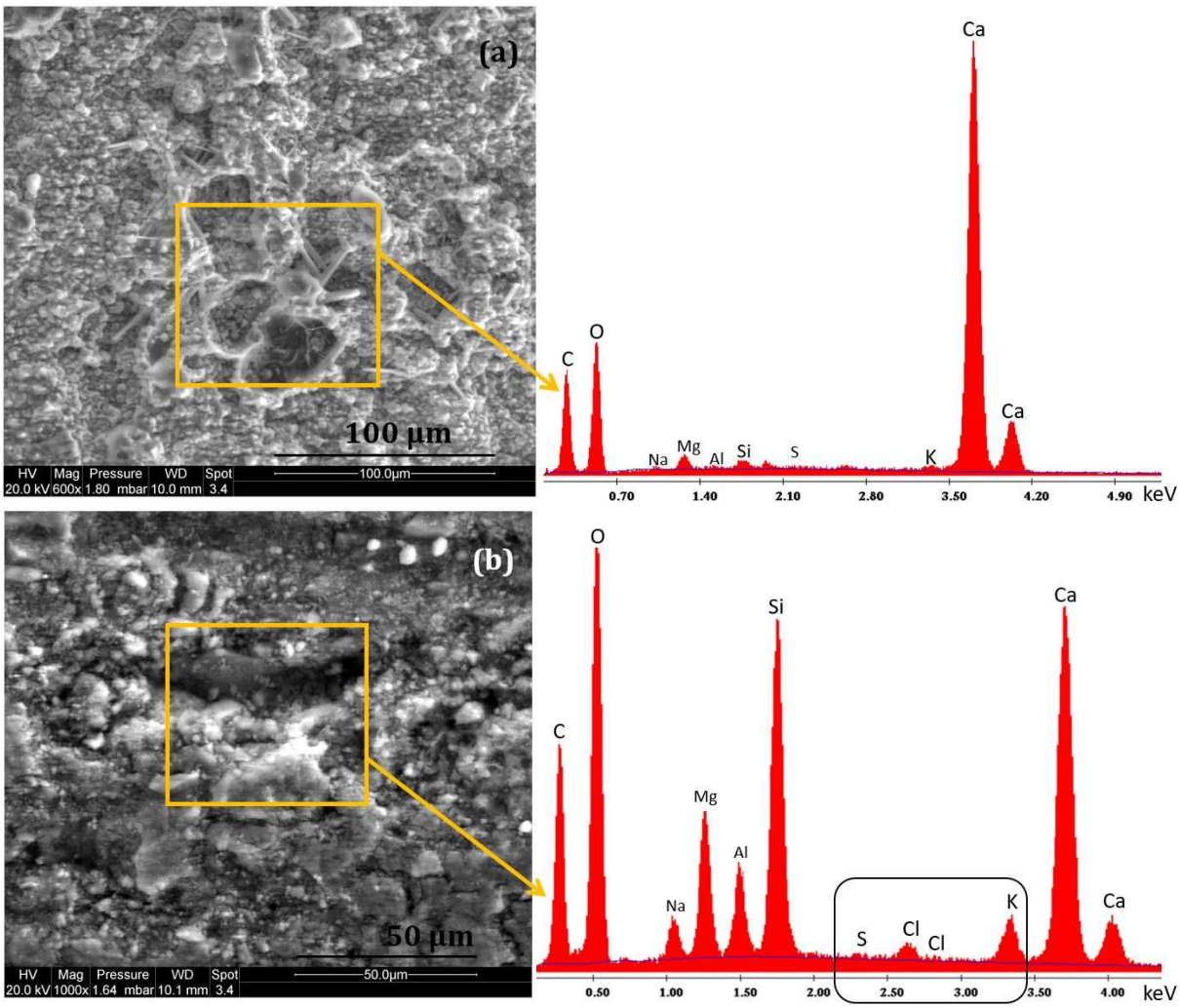

Fig. 9.SEM images and EDX spectra of S75: (a) before and (b) after the migration test.

Table 5. Chemical composition of the solid phase in the vicinity of S75 pores (% in weight)

Element	C	O	Na	Mg	Al	Si	S	Ca	Cl	K
Before migration test	15.76	31.87	0.25	0.95	0.24	0.57	0.17	49.25	0	0
After migration test	24.06	34.26	1.47	4.06	2.36	8.67	0.21	19.27	0.68	2.14

3.3. Changes to upstream and downstream solutions during the migration test

To avoid leaching of the material during the migration test, the two compartments of the migration cell were filled with a basic solution considered to be similar to the pore solution (see

section 2.2.2). However, real pore solution chemistry is not so simple. It contains other divalent ions such as calcium and sulfates [60,65]. In all cases, free ions diffuse from the material to the solutions in the compartments and vice versa, under the effect of the concentration gradient and the electrical field. Chlorides and sulfates react with the remaining anhydrous cement, calcium, sodium and potassium to form products that modify porosity, as shown above. In order to quantify the ions that diffused to/from the sample, pore solution and compartment solutions were dosed regularly during the migration test before each renewal (see section 2.2.2). We present below the concentration of ions that diffused to/from upstream and downstream. The variation in sodium and potassium in the compartments (basic solution) can then be quantified, together with the calcium leached from the material to the solutions in the compartments, and therefore the amount of portlandite dissolved and the dissolution kinetics due to the thermodynamic imbalance generated can be assessed. The concentration of diffused ions as a function of time was linearly fitted in the steady state regime in order to determine the kinetics, given that it is a migration.

3.3.1. Change in the upstream solution

Chemical analyses showed that, for all cement pastes, the upstream sodium concentration decreased compared to the initial sodium concentration (525 mmol/l) with the kinetics expressed as a flux of $6.4x10^{-2}$; $5.7x10^{-2}$; $7.1x10^{-2}$; $8.6x10^{-2}$ and $9.6x10^{-2}$ $mmol.m^{-2}.s^{-1}$ for PCI, LF25, FA30, S75 and SF10, respectively (Fig. 10). Note that the sample surface was 3.1 $x10^{-3}$ m^2 and the compartment volume was 2*l*. Furthermore, the potassium concentration decreased at a flux of $5x10^{-2}$; $6.4x10^{-2}$; $5.9x10^{-2}$; $7.7x10^{-2}$ and $5.7x10^{-2}$ $mmol.m^{-2}.s^{-1}$, respectively (Fig. 11).

For S75, a steady state was reached later than for the other materials (after about 100 hours of migration). This is explained by the capacity of S75 for the electrochemical fixation of chlorides, which delays the steady state (see section 3.1) [42]. Since sodium ions are attracted

by chlorides, their steady state could be delayed until chloride fixation is stabilized. That is why a linear trend line was considered after 100 hours (flux in steady state). Also, for the Na flux of SF10, a disturbance of the upstream sodium concentration was noted. It is known for the SF10 microstructure that the dissolution of silica forms negative charges which are neutralized by alkalis [66]. Alkalis are adsorbed on the silica surface [67]. During chloride migration and the thermodynamic disequilibrium, it seems that these alkalis could participate in the stabilization of the thermodynamic equilibrium. This could disturb the sodium concentration in the pore solution as well as its diffusivity and concentration upstream. More investigations will be necessary to confirm this explanation.

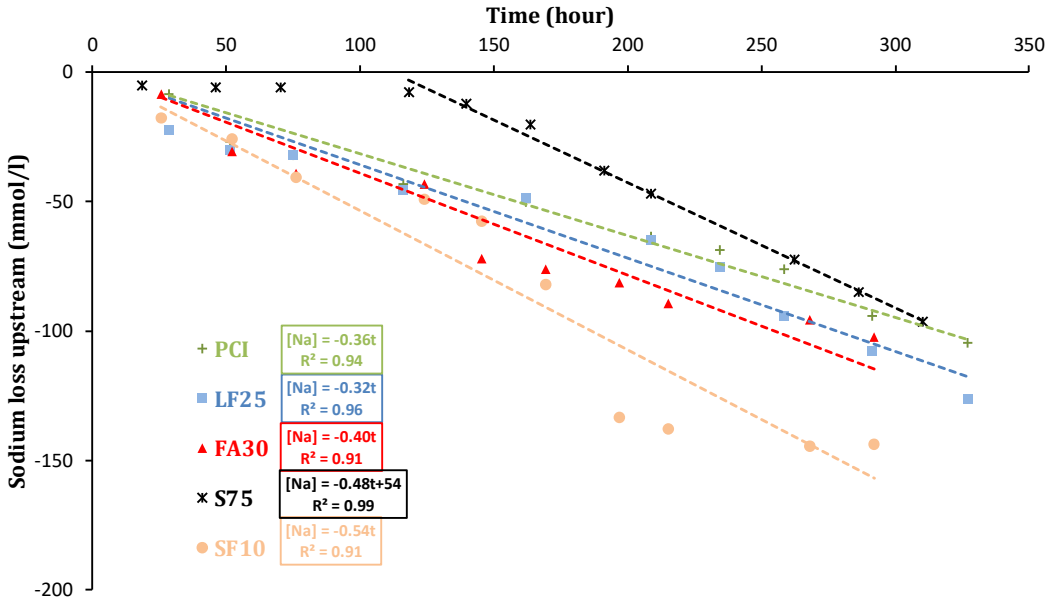

Fig. 10. Sodium loss upstream during the migration test.

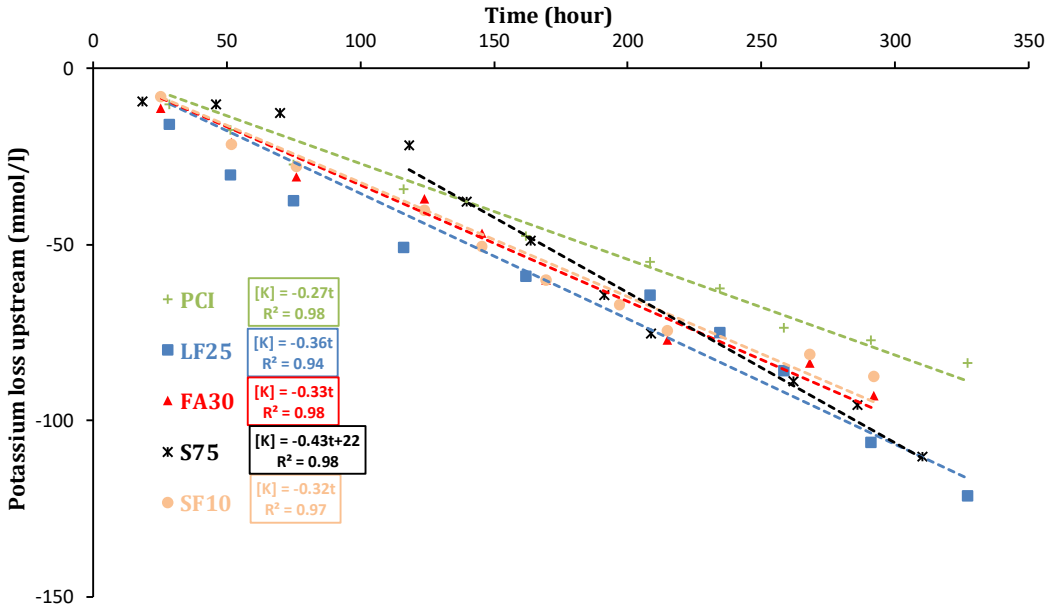

Fig. 11. Potassium loss upstream during the migration test.

An increase in upstream calcium concentration was noticed. In order to determine the source of this leached calcium, the initial calcium concentration of the material's pore solution was also dosed (after extraction) and compared to the cumulative concentration leached upstream during the migration test (Fig. 12). Note that leached downstream calcium was found to be negligible.

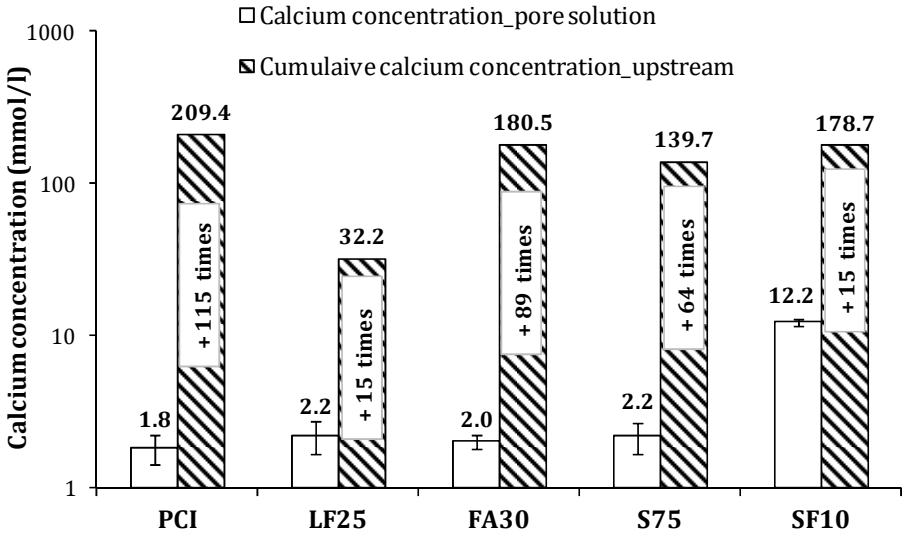

Fig. 12. Comparison between cumulative calcium concentration leached upstream during the migration test and the calcium concentration of the pore solutions.

Firstly, the quantity of calcium in PCI, LF25, FA30 and S75 was similar (~2 mmol/l). However, the quantity of calcium in SF10 was higher, despite the pozzolanic reaction of silica fume,

which consumes calcium by the silanol groups (chemisorption) or by silice to form C-S-H [68]. Andersson *et al*. [60] showed that the calcium concentration in the pore solution of cement paste with silica fume is higher than those containing Portland cement, blast furnace slag or fly ash. This is in accordance with our results. Moreover, the results showed that the cumulative calcium concentration leached at the end of the test, i.e. after 12 – 14 days, ranged from 32.2 to 209.4 mmol/l. These concentrations are higher than the initial ones in the pore solution for the corresponding pastes. They are about 115, 15, 89, 64 and 15 times higher for PCI, LF25, FA30, S75 and SF10, respectively. This excess calcium was due to the dissolution of portlandite caused by cation leaching under the electrical field and chloride migration to stabilize the thermodynamic system. Calcium ions leach subsequently upstream. The quantity of calcium in the upstream compartment, leached from LF25, was lower than those of the other cement pastes, PCI, FA30, S75 and SF10. The decalcification of cementitious materials generally involves the dissolution of Portlandite and part of C-S-H [69]. Given that limestone filler is chemically inert when used in cementitious materials [70], the low quantity of leached calcium can be assigned to, on the one hand, a smaller amount of hydrates (Portlandite and C-S-H) that can dissolve and release calcium, and on the other hand, to the use of limestone filler, where a high level (more than 20%), as in our case, can lead to the formation of monocarboaluminates and hemicarboaluminates with a consumption of Portlandite [69] and thus a decrease in the amount of calcium that can leach from the material.

Moreover, the cumulative calcium concentration with time and the kinetics of the increase in upstream calcium during the migration test are given in Fig. 13. The results could account for the kinetics of portlandite dissolution, taking into account the sample size tested, the limited amount of portlandite and supposing that the excess calcium derived only from the portlandite, according to [71]. The kinetics expressed as a flux were $1.2x10^{-1}$; $1.8x10^{-2}$; $1.1x10^{-1}$; $9.1x10^{-2}$ and $1.2x10^{-1}$ $mmol.m^{-2}.s^{-1}$ for PCI, LF25, FA30, S75 and SF10, respectively.

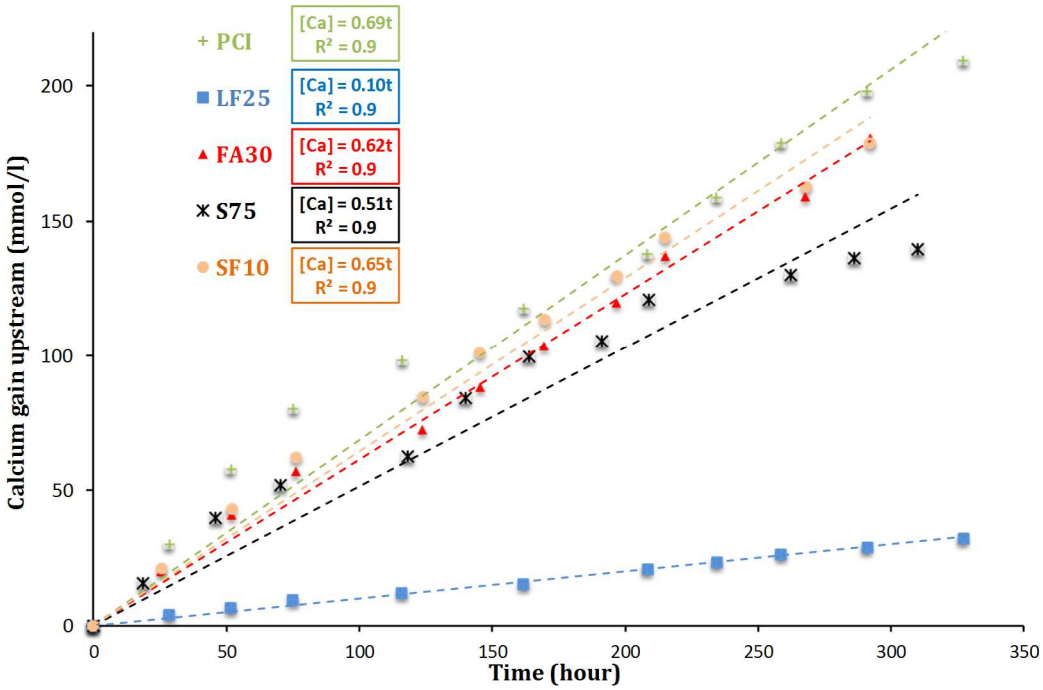

Fig. 13. Cumulative calcium concentration leached upstream during the migration test and leaching kinetics.

Furthermore, the molar concentration of upstream calcium that was released from the material represented the molar concentration of portlandite dissolved during the migration test. Indeed, the calcium released was calculated from the cumulative calcium leached as shown in Fig. 13 and the upstream volume (2*l*). The amount of portlandite dissolved in the pore solution (for a sample volume of 87 cm^3) that can modify the microstructure can then be calculated (Table 6).

Calcium released (*mmol*) = Portlandite dissolved (*mmol*) = Cumulative calcium concentration upstream (*mmol/l*) x Upstream Volume (2*l*).

Table 6. Quantity of portlandite dissolved during the migration test.

Materials	Sample volume (cm^3)	Cumulative calcium concentration (mmol/l)	Calcium released amount (mmol)	Portlandite dissolved amount (mmol)
PCI	87	209.4	418.8	418.8
LF25	87	32.2	64.4	64.4
FA30	87	180.5	361	361
S75	87	139.7	279.4	279.4
SF10	87	178.7	357.4	357.4

In reality the total quantity of portlandite dissolved during the migration test was higher, taking into account the fact that calcium could react with the other species to form new compounds in the porosity. It would also be interesting to determine the quantity and volume of new compounds formed in the porosity during chloride migration in order to compare with porosity closure shown in section 3.2. Finally, it should be noted that the sulfate concentration upstream was very low compared to the other ions.

3.3.2. Change in the downstream solution

The same approach was followed for the downstream solution before each renewal. The calcium concentration remained very low compared to the other ions it was not analyzed, and this section focuses only on sodium, potassium and sulfates. A low variation in downstream sodium concentration during the migration test was noted, apart from LF25 (Fig. 14). For this material, sodium decreased at $1.1x10^{-2}$ $mmol.m^{-2}.s^{-1}$ (the downstream volume was 1*l*). The sodium that is supposed to migrate from downstream to upstream, under the electrical field, tends to be balanced by the sodium attracted downstream by chlorides under electrostatic forces. However, downstream potassium concentration decreased compared to the initial concentration of 83 mmol/l. Indeed, potassium fluxes from downstream to the material under the electrical field were $1.8x10^{-2}$; $3.2x10^{-2}$; $2.3x10^{-2}$; $3.4x10^{-2}$ and $3.2x10^{-2}$ $mmol.m^{-2}.s^{-1}$ for PCI, LF25, FA30, S75 and SF10, respectively.

In a migration cell with only NaOH in the two compartments (unlike our migration test where there was both NaOH and KOH), Andrade [52] noted an eventual potassium leaching from the material to the compartments under a concentration gradient. Furthermore, sodium (supposed to be in equilibrium between the material and the compartments) diffused from downstream (cathode) to upstream (anode) under the electrical field. In this work, we observed a reduction in alkalis (sodium and potassium) downstream, which was explained by their migration upstream under the electrical field. However, the same reduction upstream was also noted. This could be explained by an eventual alkali attraction by chlorides, which diffuse from upstream to downstream, under the electrostatic force. Finally, from these analyses and the principle of conservation (since the migration cell is a closed environment), these results highlight an increase in alkalis in the material, which participates in the precipitation of new compounds, as indicated above in the discussion of the MEB results and the EDX spectra. More investigations on the pore solution of the materials after the migration test should be performed to complete these results.

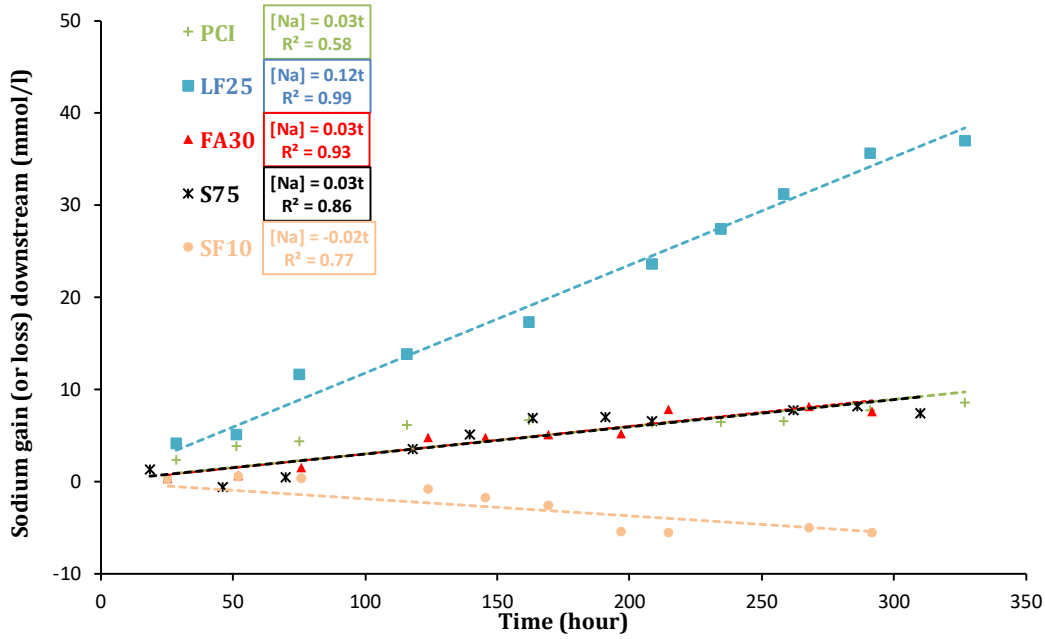

Fig. 14. Variation in downstream sodium during the migration test.

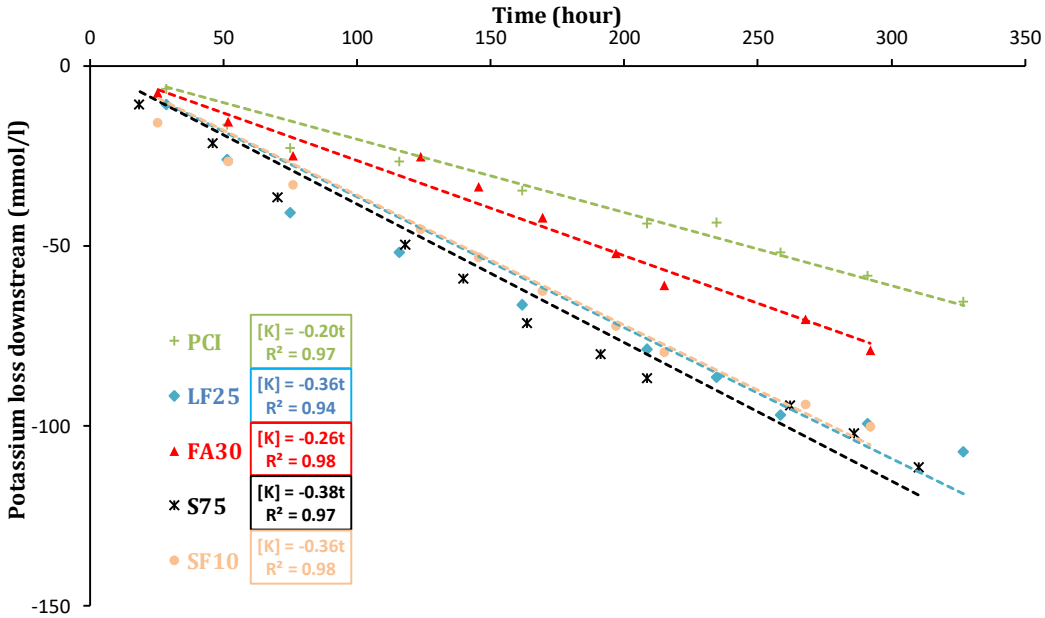

Fig. 15. Potassium loss downstream during the migration test.

Fig. 16 shows the cumulative concentration of downstream sulfates and pore solutions. The quantity of sulfates leached downstream was low relative to the calcium leached upstream. It ranged from 0.1 mmol for PCI to 1.9 mmol for SF10. The latter had the highest amount of leached sulfates because of the chemical composition of its pore solution, which is rich in sulfates (6.7 mmol/l) compared to the other materials. The partial substitution of cement by silica fumes significantly increased the concentration of sulfates in the pore solution. This is

due: (i) to the chemical composition of the silica fume used, which is high in sulfates compared to the pozzolanic and limestone additions (see Table 1); (ii) to the hydration mechanism of the cement and silica fume that slows or stops the initial formation of ettringite (sulfate consumption), although the quantity of anhydrous cement and SO_4^{2-} in the pore solution remained significant [72].

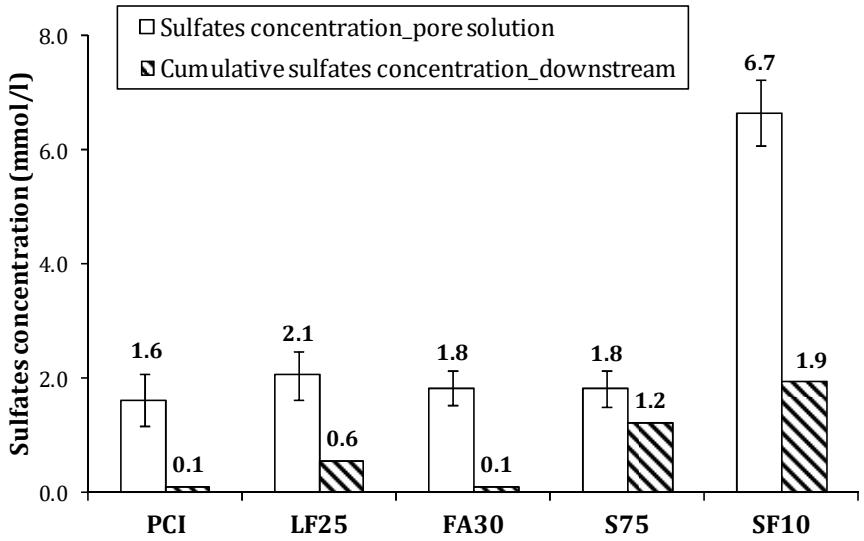

Fig. 16. Comparison between the concentration of sulfates in pore solutions (before the migration test) and the cumulative concentration of sulfates leached downstream after the migration test.

4. Conclusion

The objective of this study was to investigate the change in the microstructure and pore solution of cement pastes induced by chloride transport and the chemical interaction with anhydrous cement and hydrates during a migration test. It should be noted that the same physical and chemical interactions of chlorides with cementitious material, which influences the microstructure, can occur during the migration or natural diffusion of chloride, but with different kinetics. Additional investigations on materials immersed in a salt solution without the use of an electric field may complete the following conclusions:

- The porosity and critical pore diameter of all materials were significantly reduced, by up to 60% for porosity and 88% for critical pore diameter, except for S75, whose critical

pore diameter was initially smaller than those of the other materials and remained broadly unchanged after the migration test.

- During the chloride migration test, new compounds based on chlorides, potassium and sulfates were formed in the sample. According to the MIP results, these compounds occupied the porosity of the material in the range of 10 - 69; 15 - 50; 7 – 45 and 8 - 69 nm for PCI, LF25, FA30 and SF10, respectively.
- During the migration test, chlorides attract sodium and potassium, with the kinetics expressed as a flux of $5.7x10^{-2}$ to $9.6x10^{-2}$ and $5x10^{-2}$ to $7.7x10^{-2}$ $mmol.m^{-2}.s^{-1}$, respectively, from the upstream to the sample, due to electrostatic forces. Furthermore, potassium flux from downstream to the sample ranged from $1.8x10^{-2}$ to $3.4x10^{-2}$ $mmol.m^{-2}.s^{-1}$for the tested materials.
- Calcium in the pore solution diffused to the upstream compartment at a flux ranging between $1.8x10^{-2}$ and $1.2x10^{-1}$ $mmol.m^{-2}.s^{-1}$. This investigation estimated the amount of portlandite dissolved in cement pastes exposed to chloride (12 – 14 days of a chloride migration test), which was about 418.8, 64.4, 361, 279.4 and 357.4 mmol for a sample of 87 cm^3 of PCI, LF25, FA30, S75 and SF10, respectively.
- Sulfates in the pore solution diffused to the downstream compartment mainly for cement pastes with silica fumes that contained a high initial amount of sulfates (6.7 mmol/l in the pore solution). The amount of leached sulfates for SF10 was about 28% of the initial concentration in the pore solution.

These changes in microstructure and pore solution will in turn modify the multispecies diffusivity through cement-based materials induced by chloride transport. This highlights the importance of considering changes to the microstructure and pore solution as well as thermodynamic equilibria in modeling the transfer phenomena and diffusivity of reinforcement coatings for better accuracy in describing chloride transport and then predicting the durability

of reinforced concrete structures. Finally, it would be interesting to dose the pore solution of the tested material before and after the migration test and compare with the quantity of ions that diffused to/from the material. Furthermore, a comparison between porosity changes shown in this paper and the volume of dissolved/formed compounds may be of great interest.

Declaration of interest: This research did not receive any specific grant from funding agencies in the public, commercial or not-for-profit sectors.

Acknowledgments: The authors would like to thank the Poitou-Charentes Region (now part of the Nouvelle Aquitaine Region) and the Operational Program CPER-FEDER ("Bâtiment durable", Axis 2 "MADUR") 2014-2020 for funding this work.

5. References

[1] X. Shi, N. Xie, K. Fortune, J. Gong, Durability of steel reinforced concrete in chloride environments: An overview, Constr. Build. Mater. 30 (2012) 125–138.

[2] M. Zahedi, A.A. Ramezanianpour, A.M. Ramezanianpour, Evaluation of the mechanical properties and durability of cement mortars containing nanosilica and rice husk ash under chloride ion penetration, Constr. Build. Mater.78 (2015) 354–361.

[3] A. Balapour, E. Ramezanianpour, E. Hajibandeh, An investigation on mechanical and durability properties of mortars containing nano and micro RHA, Constr. Build. Mater. 132 (2017) 470-477.

[4] W.J. Weiss, O.B. Isgor, A.T. Coyle, C. Qiao, Prediction of chloride ingress in saturated concrete using formation factor and chloride binding isotherm, Adv. Civ. Eng. Mater. 7 (2018) 206-220.

[5] A.A Ramezanianpour, S.A Ghoreishian, B. Ahmadi, M. Balapour, A.M. Ramezanianpour, Modeling of chloride ions penetration in cracked concrete structures exposed to marine environments, Struct. Concrete. 19 (2018) 1460-1471.

[6] C. Qiao, P. Suraneni, J. Weiss, Damage in cement pastes exposed to NaCl solutions, Constr. Build. Mater. 171 (2018) 120-127.

[7] C.A. Apostolopoulos, V.G. Papadakis, Consequences of steel corrosion on the ductility properties of reinforcement bar, Constr. Build. Mater. 22 (2008) 2316–2324.

[8] V.A. Franco-Luján, M.A. Maldonado-García, J.M. Mendoza-Rangel, P. Montes-García, Chloride-induced reinforcing steel corrosion in ternary concretes containing fly ash and untreated sugarcane bagasse ash, Constr. Build. Mater.198 (2019) 608–618.

[9] O. Amiri, H. Friedmann, A. Aït-Mokhtar, Modelling of chloride-binding isotherm by multi-species approach in cement mortars submitted to migration test, Mag. Concr. Res. 58 (2006) 93–99.

[10] L. Sutter, K. Peterson, S. Touton, T. Van Dam, D. Johnston, Petrographic evidence of calcium oxychloride formation in mortars exposed to magnesium chloride solution, Cem. Concr. Res. 36 (2006) 1533–1541.

[11] O. Amiri, A. Aït-Mokhtar, P. Dumargue, G. Touchard, Electrochemical modelling of chloride migration in cement-based materials. Part I. Theoretical basis at microscopic scale, Electrochim Acta 46 (2001) 1267–1275.

[12] H. Friedmann, O. Amiri, A. Aït-Mokhtar, Physical modeling of the electrical double layer effects on multispecies ions transport in cement-based materials, Cem. Concr. Res. 38 (2008) 1394–1400.

[13] O. Omikrine Metalssi, A. Aït-Mokhtar, P. Turcry, B. Ruot, Consequences of carbonation on microstructure and drying shrinkage of a mortar with cellulose ether, Constr. Build. Mater. 34 (2012) 218–225.

[14] P. Turcry, L. Oksri-Nelfia, A. Younsi, A. Aït-Mokhtar, Analysis of an accelerated carbonation test with severe preconditioning, Cem. Concr. Res. 57 (2014) 70-78.

[15] T. Mauroux, F. Benboudjema, P. Turcry, A. Aït-Mokhtar, O. Deves, Study of cracking due to drying in coating mortars by digital image correlation, Cem. Concr. Res. 42 (2012) 1014–1023.

[16] S. Chatterji, Mechanism of the $CaCl_2$ attack on Portland cement concrete, Cem. Concr. Res. 8 (1978) 461–467.

[17] F.P. Glasser, J. Pedersen, K. Goldthorpe, M. Atkins, Solubility reactions of cement components with NaCl solutions: I. Ca(OH) 2 and C-S-H', Adv. Cem. Res. 17 (2005) 57–64.

[18] A.K. Suryavanshi, J.D. Scantlebury, S.B. Lyon, Mechanism of Friedel's salt formation in cements rich in tri-calcium aluminate, Cem. Concr. Res. 26, (1996) 717–727.

[19] A. Mesbah, M. François, C. Cau-dit-Coumes, F. Frizon, Y. Filinchuk, F. Leroux, J. Ravaux, G. Renaudin, Crystal structure of Kuzel's salt $3CaO{\cdot}Al_2O_3{\cdot}1/2CaSO_4{\cdot}1/2CaCl_2{\cdot}11H_2O$ determined by synchrotron powder diffraction, Cem. Concr. Res. 41 (2011) 504–509.

[20] H.G. Midgley, J.M. Illston, The penetration of chlorides into hardened cement pastes, Cem. Concr. Res. 14 (1984) 546–558.

[21] O.A. Kayyali, M.N. Haque, Chloride penetration and the ratio of Cl^-/OH^- in the pores of cement paste, Cem. Concr. Res. 18 (1988) 895–900.

[22] M. Regourd, H. Hornain, B. Montureux, Microstructure of Concrete in Aggressive Environments, 1st Int. Conf. on Durability of Building Materials and Components. Nat. Res. Council Canada, Ottawa, 1978.

[23] D.A. Koleva, J. Hu, A.L. A. Fraaij, K. van Breugel, J.H.W. de Wit, Microstructural analysis of plain and reinforced mortars under chloride-induced deterioration, Cem. Concr. Res. 37 (2007) 604–617.

[24] X. Hu, C. Shi, Q. Yuan, J. Zhang, G. De Schutter, Influences of chloride immersion on zeta potential and chloride concentration index of cement-based materials', Cem. Concr. Res. 106 (2018) 49–56.

[25] A. Aït-Mokhtar, O. Poupard, P. Dumargue, Relationship between the transfer properties of the coating and impedance spectroscopy in reinforced cement-based materials, J. Mater. Sci. 41 (2006) 6006-6014.

[26] A. Hamami, J.M. Loche, A. Aït-Mokhtar, Cement fraction effect on EIS response of chloride migration tests, Adv. Cem. Res. 23 (2011) 233–240.

[27] I. Sànchez, X.R. Novoa, G. de Vera, M.A. Climent, Microstructural modifications in Portland cement concrete due to forced ionic migration tests. Study by impedance spectroscopy, Cem. Concr. Res. 38 (2008) 1015–25.

[28] L. Tang, Concentration dependence of diffusion and migration of chloride ions: Part 1. Theoretical considerations, Cem. Concr. Res.29 (1999) 1463–1468.

[29] L. Tang, Concentration dependence of diffusion and migration of chloride ions: Part 2. Experimental evaluations, Cem. Concr. Res. 29 (1999) 1469–1474.

[30] M. Castellote, C. Andrade, C. Alonso, Measurements of the steady and non-steady-state chloride diffusion coefficients in a migration test by means of monitoring the conductivity in the anolyte chamber. Comparison with natural diffusion tests, Cem. Concr. Res. 31 (2001) 1411–1420.

[31] C.T. Chiang, C.C. Yang, Relation between the diffusion characteristic of concrete from salt ponding test and accelerated chloride migration test, Mater. Chem. Phys. 106 (2007) 240–246.

[32] M. Castellote, C. Andrade, C. Alonso, Changes in concrete pore size distribution due to electrochemical chloride migration trials, ACI Mater. J. 96 (1999) 314–319.

[33] L. Majlbro, The complete solution of Fick‘s second law of diffusion with time dependent diffusion coefficient and surface concentration, Durab. Concr. Saline Environ, Cementa AB, Dandcryd Sweden (1996) 127–158.

[34] O. Amiri, A. Aït-Mokhtar, A. Seigneurin, A complement to the discussion of A. Xu and S. Chandra about the paper «Calculation of chloride coefficient diffusion in concrete from ionic migration measurements» by C. Andrade, Cem. Concr. Res. 27 (1997) 951– 957.

[35] J. Xia, L. Li, Numerical simulation of ionic transport in cement paste under the action of externally applied electric field, Constr. Build. Mater. 39 (2013) 51–59.

[36] L. Jiang, Z. Song, H. Yang, Q. Pu, Q. Zhu, Modeling the chloride concentration profile in migration test based on general Poisson Nernst Planck equations and pore structure hypothesis, Constr. Build. Mater. 40 (2013) 596–603.

[37] M.M. Jensen, K. De Weerdt, B. Johannesson, M.R. Geiker, Use of a multi-species reactive transport model to simulate chloride ingress in mortar exposed to NaCl solution or sea-water, Comput. Mater. Sci. 105 (2015) 75–82.

[38] L. Mao, Z. Hu, J. Xia, G. Feng, I. Azim, J. Yang, Q. Liu, Multi-phase modelling of electrochemical rehabilitation for ASR and chloride affected concrete composites, Compos. Struct. 207 (2019) 176–189.

[39] NF EN 197-1, Ciment – Partie 1: Composition, spécifications et critères de conformité des ciments courants, 2012.

[40] M.I.A. Khokhar, E. Roziere, P. Turcry, F. Grondin, A. Loukili, Mix design of concrete with high content of mineral additions: Optimisation to improve early age strength, Cem. Concr. Compos. 32 (2010) 377–385.

[41] A. Younsi, P. Turcry, E. Rozière, A. Aït-Mokhtar, A. Loukili, Performance-based design and carbonation of concrete with high fly ash content, Cem. Concr. Compos. 33 (2011) 993–1000.

[42] R.K. Dhir, M.A.K. El-Mohr, T. D. Dyer, Chloride binding in GGBS concrete, Cem. Concr. Res. 26 (1996) 1767–1773.

[43] A.L. Fraay, J. Bijen, Y. de Haan, The reaction of fly ash in Concrete. A critical Examination, Cem. Conc. Res. 19 (1989) 235–246.

[44] D. Perraton, P. Aïtcin, D. Vezena, Permeability of Silica Fume Concrete, Am. Concr. Inst. 108 (1988) 63–84.

[45] O. Truc, J.P. Ollivier, M. Carcassès, A new way for determining the chloride diffusion coefficient in concrete from steady state migration test, Cem. Concr. Res. 30 (2000) 217–226.

[46] NF P18-459, Concrete – Testing hardened concrete – Testing porosity and density, 2010.

[47] S. Diamond, Aspects of concrete porosity revisited, Cem. Concr. Res. 29 (1999) 1181–1188.

[48] S. Diamond, Mercury porosimetry. An inappropriate method for the measurement of pore size distributions in cement-based materials, Cem. Concr. Res. 30 (2000) 1517–1525.

[49] A. Aït-Mokhtar, O. Amiri, P. Dumargue, A. Bouguerra, On the applicability of washburn law: study of mercury and water flow properties in cement-based materials, Mater. Struct. 37 (2004) 107–113.

[50] L. Divet, R. Randriambololona, Delayed Ettringite Formation: The Effect of Temperature and Basicity on the Interaction of Sulphate and C-S-H Phase 1, Cem. Concr. Res. 28 (1998) 357–363.

[51] A. Aït-Mokhtar, O. Amiri, O. Poupard, P. Dumargue, A new method for determination of chloride flux in cement-based materials from chronoamperometry, Cem. Concr. Compos. 26 (2004) 339–345.

[52] C. Andrade, Calculation of chloride diffusion coefficients in concrete from ionic migration measurements, Cem. Concr. Res. 23 (1993) 724–742.

[53] O. Amiri, A. Aït-Mokhtar, P. Dumargue, Optimisation de l'exploitation de l'essai d'électrodiffusion d'ions chlorure dans le béton. Revue Française de Génie Civil, 4 (2000) 161– 173.

[54] P. Longuet, L. Burglen, A. Zelwer, The liquid phase of hydrated cement, Rev. Mater. Constr. 676 (1973) 35-41.

[55] R.S. Barneyback, S. Diamond, Expression and analysis of pore fluids from hardened cement pastes and mortars, Cem. Concr. Res. 11 (1981) 279–285.

[56] A. /kDureković, Cement pastes of low water to solid ratio: An investigation of the porosity characteristics under the influence of a superplasticizer and silica fume, Cem. Concr. Res. 25 (1995) 365–375.

[57] D. Kong, X. Du, S. Wei, H. Zhang, Y. Yang, S.P. Shah, Influence of nano-silica agglomeration on microstructure and properties of the hardened cement-based materials, Constr. Build. Mater. 37 (2012) 707–715.

[58] T.D. Marcotte, C.M. Hansson, B.B. Hope, The effect of the electrochemical chloride extraction treatment on steel-reinforced mortar. Part II. Microstructural characterization, Cem. Concr. Res. 29 (1999) 1561–1568.

[59] G.W. Scherer, Crystallization in pores, Cem. Conc. Res. 29 (1999) 1347–1358.

[60] K. Andersson, B. Allard, M. Bengtsson, B. Magnusson, Chemical composition of cement pore solutions, Cem. Concr. Res. 19 (1989) 327–332.

[61] D. Damidot, F.P. Glasser, Thermodynamic investigation of the CaO-Al_2O_3 $CaSO_4$-H_2O system at 50°C and 85°C, Cem. Concr. Res. 22 (1992) 1179–1191.

[62] S. Monosi, M. Collepardi, Research on $3CaO \cdot CaCl_2 \cdot 15H_2O$ identified in concretes damaged by $CaCl_2$ attack, I1 Cimento, 87 (1990) 3–8.

[63] C. Famy, K.L. Scrivener, A. Atkinson, A.R. Brough, Effects of an early or a late heat treatment on the microstructure and composition of inner C-S-H products of Portland cement mortars, Cem. Concr. Res. 32 (2002) 269–278.

[64] F.P. Glasser, The role of sulphate mineralogy cue temperature in delayed ettringite formation, Cem. Concr. Compos. 18 (1996) 187–193.

[65] Y. Xu, The influence of sulphates on chloride binding and pore solution chemistry, Cem. Concr. Res. 27 (1997) 1841–1850.

[66] L.S. Dent Glasser, N. Kataoka, The chemistry of "alkali-aggregate" reaction, Cem. Concr. Res. 11 (1981) 1-9.

[67] S. Urhan, Alkali silica and pozzolanic reactions in concrete. Part 1: Interpretation of published results and an hypothesis concerning the mechanism, Cem. Concr. Res. 17 (1987) 141-152.

[68] S.A. Greenberg, The chemisorption of calcium hydroxide by silica, J. Phys. Chem. 60 (1956) 325-330, 1956.

[69] S. Catineaud, J.J. Beaudoin, J. Marchand, Influence of limestone addition on calcium leaching mechanisms in cement-based materials, Cem. Concr. Res. 30 (2000) 1961-1968.

[70] G. Ye, X. Liu, G. De Schutter, A.M. Poppe, L. Taerwe, Influence of limestone powder used as filler in SCC on hydration and microstructure of cement pastes, Cem. Concr. Compos. 29 (2007) 94–102.

[71] V.Q. Tran, A. Soive, V. Baroghel-Bouny, Modelisation of chloride reactive transport in concrete including thermodynamic equilibrium, kinetic control and surface complexation, Cem. Concr. Res. 110 (2018) 70–85.

[72] C. Lobo, M.D. Cohen, Hydration of type K expansive cement paste and the effect of silica fume: II. Pore solution analysis and proposed hydration mechanism, Cem. Concr. Res. 23 (1993) 104–114.